Modulated desynchronism in short pulse free-electron laser oscillators

Oscar G. Calderón,* Takuji Kimura, and Todd I. Smith
Stanford Picosecond FEL Center, Hansen Experimental Physics Laboratory, Stanford University, Stanford, California 94305-4085
(Received 24 February 2000; published 18 September 2000)

We present an experimental and theoretical study of the effect of desynchronism modulation on short pulse free-electron laser (FEL) oscillators. We find that the output power and the micropulse length of the FEL beam oscillate periodically at the modulation frequency and that the minimum micropulse length during the cycle can be significantly shorter than that which can be obtained without modulation. For example, when the desynchronism of our FEL is modulated at 40 kHz, the minimum measured micropulse length is 300 fs. Without modulation the minimum is about 700 fs. We show that when the desynchronism is modulated, the FEL can operate for part of the cycle in the normally inaccessible portion of the output power curve where the FEL gain is less than the cavity losses. It is even possible for the FEL to operate periodically in the region of negative desynchronism where gain, as normally defined, does not exist.

PACS numbers: 41.60.Cr, 42.60.Jf, 42.65.Re, 42.65.Sf

I. INTRODUCTION

In a free-electron laser (FEL), a relativistic electron beam passes through the periodic transverse magnetic field of an undulator (or a wiggler), transferring energy to a copropagating electromagnetic wave. The electron beam, after traveling N_w wiggler periods, lags behind the optical beam a slippage distance $L_s = \lambda N_w$, where $\lambda = \lambda_w(1 + a_w^2)/(2\gamma_0^2)$ is the resonance wavelength of the radiation, with λ_w and a_w the wiggler period and rms parameter, respectively, and γ_0 is the initial electron energy in mc^2 units. In pulsed FEL oscillators, successive electron pulses periodically enter the wiggler, where they copropagate with the stored optical pulse. When the slippage distance is comparable with or larger than the electron pulse length (L_b), longitudinal overlap effects dominate the FEL dynamics. By varying the desynchronism between the periodic beam injection and the round-trip time of the radiation in the cavity, it is possible to control the overlap between the radiation and the electron pulses during many round-trips. In fact, a finite desynchronism $\delta\mathcal{L}$ is necessary to maintain synchronism between electron and optical pulses in the cavity because of the effect of laser lethargy [1], which causes the centroid of the optical pulse to travel slower than the speed of light in vacuum.

During the past few years there has been much interest in the topic of generating and controlling short FEL pulses [2–8]. To date, short pulse generation has been achieved while maintaining the two fundamental FEL parameters (the cavity detuning $\delta\mathcal{L}$ and the losses introduced by the cavity α_0) constant. In this paper we show that modulating $\delta\mathcal{L}$ provides a new method of controlling the pulse length of an FEL [9,10]. Previous studies on the effects of dynamic desynchronism by Jaroszynski *et al.* [11,12] and Bakker *et al.* [4] have demonstrated the utility of the technique in switching an FEL rapidly between high gain and high power regimes. In the present work we explore the observation that when $\delta\mathcal{L}$ is modulated by a few microns at a 40 kHz rate, the measured micropulse length of our FEL varies as a function of the phase relative to the modulation from a minimum of 300 fs to a maximum of 800 fs. When the modulation is turned off, the micropulse length is about 700 fs. These measurements were made at a wavelength of 5 μm using a time-synchronized measurement of the micropulse length, the optical power spectrum, and the optical power as a function of the phase of the modulating signal.

This paper is organized as follows. In Sec. II the experimental setup and measurement results are presented, followed by a brief discussion. In Sec. III A we describe the theoretical model which consists of the oscillator equations for a short pulse FEL with a time periodic cavity detuning. Comparisons of the experimental and the theoretical results are shown in Secs. III B and III C for the cases without and with modulation, respectively. In the set of equations we use, we keep two terms that are usually discarded in the description of this type of FEL. In Sec. III D we analyze the effect of including those two terms. The final conclusions are given in Sec. IV.

II. EXPERIMENT

A. Experimental setup and results

The FEL beam line at the Stanford FEL consists mainly of four accelerator structures and two FEL undulators. The first two structures accelerate the beam to approximately 20 MeV. After passing through the magnetic chicanes of a far-infrared FEL, the beam undergoes further acceleration by two more structures before entering the $N_w = 72$

*Permanent address: Dept. Optica, Facultad de Ciencias Físicas, Universidad Complutense, Cuidad Universitaria s/n, 28040 Madrid, Spain.

period mid-infrared FEL undulator ($\lambda_w = 3.1$ cm). The rms wiggler parameter is $a_w = eB_w\lambda_w/2\pi mc = 0.83$. During typical FEL operation, the wavelength of the mid-infrared beam is stabilized through a feedback loop on the first accelerating structure. By opening this loop and applying signals from a function generator, the energy of the electron beam can be modulated.

The autocorrelation signal and the optical power signal are recorded as a function of time and are shown in Fig. 1. Each of the three plots corresponds to a different modulation level. Flat signals were taken without modulation and are shown for comparison. As the modulation level increases, the maximum of the autocorrelation becomes much higher than the normal level, while the change in power is less prominent. This is an indication of a decrease in the micropulse length.

By gating the signals from the autocorrelator, the spectrum analyzer, and the power detector, respectively, simultaneous measurements of the micropulse length, the spectral width, and the optical power as a function of the phase of the modulating signal can be made. Figure 2 shows one set of measurements at an energy modulation level of about 0.1% ($\Delta E \simeq 30$ keV). The measured micropulse length ranges from 300 to 800 fs (FWHM) while the spectral width varies from 2.3% to 0.9% (FWHM). The product remains transform limited throughout the entire cycle.

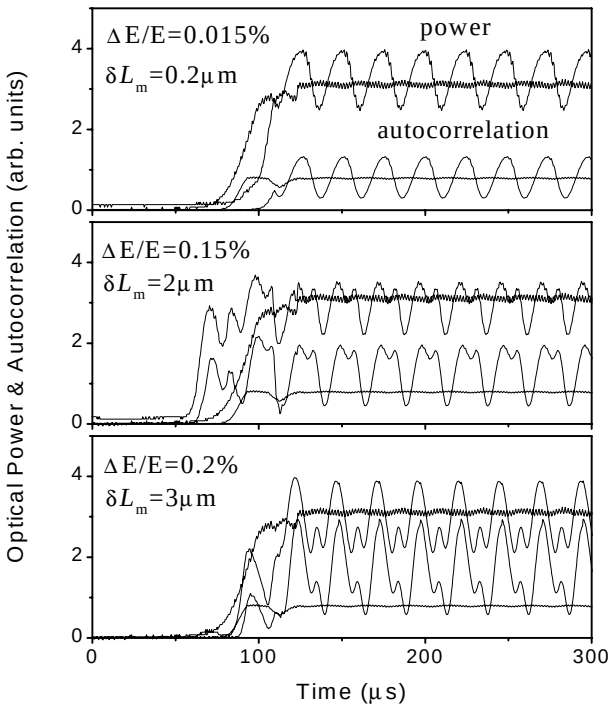

FIG. 1. Plots of autocorrelation and optical power signals as a function of time with different levels of beam energy modulation. The flat curves are for situations without the energy modulation. The average desynchronism is $\delta\mathcal{L}_0 = 1.5$ μm.

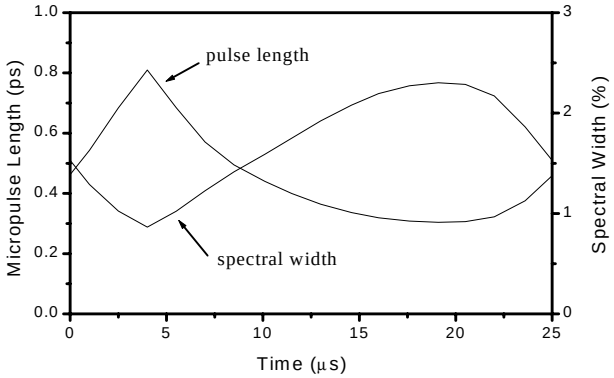

FIG. 2. Plot of micropulse length (FWHM) and spectral width (FWHM) as a function of time when the beam energy is modulated at 40 kHz. The average desynchronism is $\delta\mathcal{L}_0 = 1.5$ μm.

B. Discussion

The magnetic chicanes in the FEL beam line are non-isochronous, i.e., higher energy electrons pass through them more quickly than lower energy ones. The effect is calculated to be 0.03 ps/keV. Thus modulation of the beam energy is translated into modulation of the electron bunch repetition frequency. If we assume that the energy modulation takes the form $(\Delta E/2)\cos(2\pi f_m t)$, where ΔE is the peak-to-peak energy modulation in keV and f_m is the modulation frequency in Hz, then the fractional change in the electron bunch repetition frequency is given by

$$\frac{\Delta f}{f_{\mathrm{FEL}}} = 1.5 \times 10^{-14} 2\pi f_m \Delta E \sin(2\pi f_m t), \qquad (2.1)$$

where f_{FEL} is the nominal value of the repetition frequency ($f_{\mathrm{FEL}} = 11.8$ MHz). Since a change in the repetition frequency has the same effect as the cavity length detuning $\delta\mathcal{L}_m = L_{\mathrm{cav}}(\Delta f/f_{\mathrm{FEL}})$, an equivalent cavity length detuning can be calculated from Eq. (2.1). In our experiment, the magnitude of the energy modulation is monitored with an electric field probe inside the first accelerator structure. The energy modulation present during the measurements for Fig. 2 implies an effective cavity length modulation of about 3 μm peak to peak. This is comparable to the entire cavity length detuning curve for our FEL and seems quite likely to be responsible for the micropulse length modulation.

III. THEORY

A. Theoretical model

We use the short pulse FEL oscillator equations, which are derived and discussed in detail in Ref. [7]. In an oscillator, the radiation is reflected backward after amplification and then forward for the next pass. The input field for the $(n+1)$th pass is $A_0^{(n+1)}(\xi - \delta) = rA_f^{(n)}(\xi)$, where A_f and A_0 are the radiation fields at the end and at the entrance

of the wiggler, respectively, $\xi = (ct - z)/L_s$ is the position within the optical pulse in units of the slippage length, z is the position along the wiggler, $r = 1 - \alpha_0/2$ accounts for the reduction in amplitude due to energy losses at the mirrors, and $\delta = 2\delta\mathcal{L}/L_s$ is the normalized desynchronism. The linear gain per pass is assumed to be small, so $A_0^{(n+1)}(\xi - \delta)$ may be approximated by the following Taylor expansion:

$$A_0^{(n+1)}(\xi - \delta) \simeq A_0^{(n)}(\xi) + \frac{\partial A_0^{(n)}(\xi)}{\partial n} - \delta\frac{\partial A_0^{(n)}(\xi)}{\partial \xi} + \frac{1}{2}\frac{\partial^2 A_0^{(n)}(\xi)}{\partial n^2} + \frac{\delta^2}{2}\frac{\partial^2 A_0^{(n)}(\xi)}{\partial \xi^2}, \tag{3.1}$$

where the pass number n is considered a coarse-grained variable. The last two terms in this Taylor expansion were not taken into account in previous works [7,8]. However, as will be shown in Sec. III D, they are relevant in explaining the behavior of the system when the cavity detuning becomes very small, or even negative, values. Defining $A(\xi,\tau) = A_0^{(n)}(\xi)$, $B = \langle \exp(-i\theta)\rangle$, $D = \langle p\exp(-i\theta)\rangle$, $Q = \langle p\rangle$, and $S = \langle p^2\rangle$, with $p = \partial_\xi\theta$ and θ the electron phase, the equations are for $0 < \xi < 1$

$$\frac{\partial A}{\partial \tau} - \nu\frac{\partial A}{\partial \xi} + \frac{1}{2}\frac{\partial^2 A}{\partial \tau^2} + \frac{\gamma\nu^2 A}{\partial \xi^2} + \frac{\alpha}{2}A = B, \tag{3.2}$$

$$\frac{\partial B}{\partial \xi} = -iD, \tag{3.3}$$

$$\frac{\partial D}{\partial \xi} = -A - iSB - 2iQD + 2iQ^2 B, \tag{3.4}$$

$$\frac{\partial Q}{\partial \xi} = -[AB^* + \text{c.c.}], \tag{3.5}$$

$$\frac{\partial S}{\partial \xi} = -2[AD^* + \text{c.c.}], \tag{3.6}$$

where $\tau = \gamma n$, $\nu = \delta/\gamma$, $\alpha = \alpha_0/\gamma$, and $\gamma = (L_b/L_s)g_0$. Here g_0 is the usual cw small gain coefficient defined as $g_0 = 4\pi(N_w/\gamma_0)^3(I_b f/I_0)(a_w\lambda_w F/r_b)^2$, I_b is the peak electron current $F = J_0(s) - J_1(s)$ with $s = a_w^2/4(1 + a_w^2/2)$, r_b is the beam radius, $I_0 = 4\pi\epsilon_0 mc^3/e \simeq 17\,000$ A is the Alfvén current, and f is the filling factor describing the transverse overlap between the optical and the electron pulses. The amplitude A is chosen such that $|A|^2 = 4\pi N_w g_0 P_{\text{in}}(z,t)/Pe$, where $P_{\text{in}}(z,t)$ is the intracavity optical power and $P_e = mc^2\gamma_0(I_b/e)$ is the electron beam power.

Equations (3.2)–(3.6) have been solved numerically using the finite differences method. The initial beam is assumed to be monochromatic and unbunched, and the initial energy satisfies the FEL resonant condition. Hence the initial conditions are $B = D = Q = S = 0$ at $\xi = 0$. For $\nu < 0$ or $\nu > 0$, we assume $A(\xi = 0,\tau) = A_0$ or $A(\xi = 1,\tau) = A_0$, respectively, where A_0 characterizes the level of spontaneous emission [7,8]. The initial field is assumed to match the level of spontaneous emission, $A(\xi,\tau = 0) = A_0$. We define the dimensionless output power P and the time averaged power P_t as

$$P(\tau) = \int_0^1 d\xi\,|A(\xi,\tau)|^2, \tag{3.7}$$

$$P_t = \frac{1}{\tau_2 - \tau_1}\int_{\tau_1}^{\tau_2} d\tau\,P(\tau). \tag{3.8}$$

In the steady state case, where P is constant, both magnitudes are equal; i.e., $P_t = P$.

B. Comparison without modulated desynchronism

First, we will compare the theoretical behavior with the experimental result for the case without modulated desynchronism, i.e., with a constant detuning. The following parameters of the FEL are being used: the wiggler length $L_w = N_w\lambda_w = 2.2$ m, the radiation wavelength $\lambda = 5$ μm, the initial energy $\gamma_0 = 64.6$, the slippage $L_s = \lambda N_w = 360$ μm, the peak electron current $I_b = 13$ A, and the electron micropulse length $L_b = 390$ μm. The cavity loss was determined by fitting the falling edge of the optical macropulse to a logarithmic curve and was found to be $\alpha_0 = 0.03$.

The value for the gain parameter $\gamma = (L_b/L_s)g_0$ is chosen so that the theoretical growth rate of the optical power in the linear regime matches that of the experiment. Figure 3 compares the temporal evolution of the experimental radiation field with the theoretical prediction, using the values $\gamma = 0.283$, $g_0 = 0.26$, and $\alpha = 0.106$. Further calculation using these values gives good agreement between experiment and theory for the output power versus desynchronism (see Fig. 4) and allows us to establish absolute values for the desynchronism with reasonable precision (desynchronism values relative to an arbitrary zero can be measured with a precision of about 0.2 μm). The theoretical value of the micropulse length for the

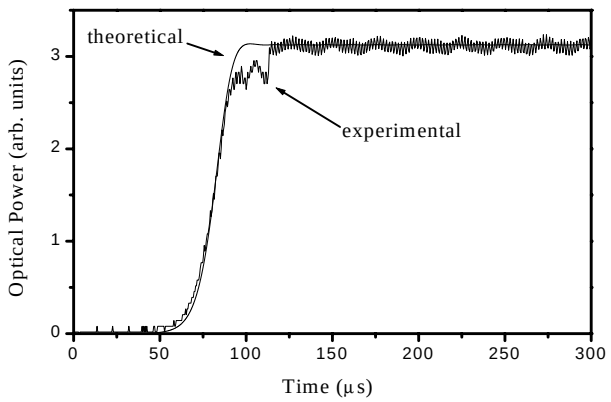

FIG. 3. Experimental and theoretical optical power time evolution for $\nu = 0.03$ ($\delta\mathcal{L} = 1.5$ μm).

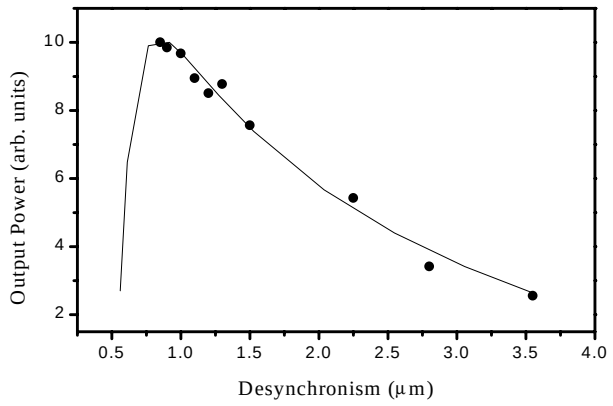

FIG. 4. Comparison between theoretical model (solid line) and experimental measurements (points) of the output power versus the desynchronism.

conditions of Fig. 3 ($\delta\mathcal{L} = 1.5\ \mu$m) is about 700 fs, in accord with experiment. The minimum calculated micropulse length ($\delta\mathcal{L} \simeq 1.0\ \mu$m) is about 600 fs, about a factor of 2 larger than the minimum measured and calculated when the desynchronism is modulated.

Because our simplified model has zero energy spread and emittance, we have introduced a phenomenological filling factor, $f = 0.34$, to account for a decrease in small signal gain. The gain parameter calculated from the definition (Sec. III A), where we assume $r_b = |L_{\rm cav}\lambda/(2\pi)|^{1/2} = 3$ mm, together with the filling factor, agrees with that calculated from the experimental data. It is interesting to note that Piovella *et al.* [7] used the same f value to compare their theory with the FELIX.

C. Comparison with modulated desynchronism

Taking into account the modulated desynchronism $\delta\mathcal{L}_m = L_{\rm cav}(\Delta f/f_{\rm FEL})$ and using Eq. (2.1)), the total cavity detuning can be written as

$$\nu = \nu_0 + \Delta\nu_m \sin\left(\frac{2\pi f_m}{\gamma f_{\rm FEL}}\,\tau\right), \tag{3.9}$$

where $\Delta\nu_m = 1.5 \times 10^{-14}(4\pi f_m L_{\rm cav}\Delta E)/\gamma L_s$. We use $f_m = 40$ kHz, which was the modulation frequency that produced the largest effect in the experiments.

The theoretical optical power signal is shown in Fig. 5 as a function of time for three different modulation levels. For small amplitude modulation we observe a modulation of the optical power at 40 kHz, the same frequency as the beam energy modulation [see Fig. 5(a)]. This is in agreement with the experiment. As the amplitude of modulation increases, a new frequency appears [see Figs. 5(b) and 5(c)]. In Fig. 6 we show $|A(\xi,\tau)|^2$ as a function of time (during one period of the modulation) and the optical pulse position ξ. Each plot corresponds to a different modulation level. For the case without modulation, $\Delta\nu_m = 0$ [see Fig. 6(a)], we can see how the pulse shape remains constant, i.e., there is a constant micropulse length around 700 fs. When the modulation

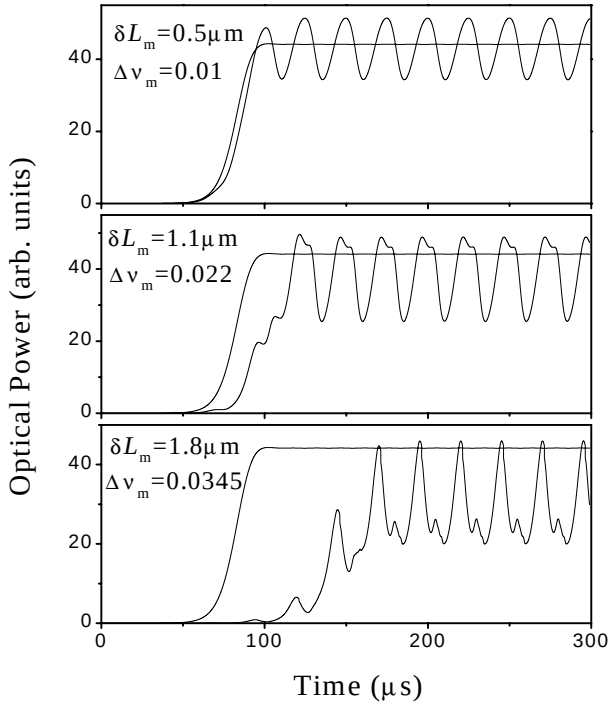

FIG. 5. Optical power signals as a function of time with different levels of beam energy modulation. The flat curves are for situations without the energy modulation. The average cavity detuning is $\nu_0 = 0.03$.

is applied, the pulse shape and the micropulse length oscillate at the modulation frequency. It shows how the pulse length reaches shorter values as the modulation amplitude increases [see Fig. 6(d)], in agreement with the experimental results. At $\Delta\nu_m = 0.0345$, calculation shows that the micropulse length varies between 300 and 800 fs.

In order to understand the role of the modulated desynchronism in FEL dynamics, we show in Fig. 7 the output power versus desynchronism curve obtained without modulation. In this figure the average cavity detuning value is shown at $\nu_0 = 0.03$. The horizontal lines represent the range of detuning values due to various modulation amplitudes. When modulation is applied, the FEL state must evolve from instant as it attempts to follow the changing conditions. It is reasonable to assume that it moves toward the steady condition corresponding to the instantaneous detuning value. Therefore, for small modulation the power will decrease as $\nu > \nu_0$ and will increase as $\nu < \nu_0$. This explains the periodicity observed in the output power. When the modulation amplitude becomes large enough [Figs. 7(b) and 7(c)], such that the detuning reaches values smaller than $\nu_{\rm max}$ (maximum output power), the equilibrium power is no longer monotonic in ν, and the output power curve develops higher frequency structure [Figs. 1, 5(b), and 5(c)].

Since the micropulse length of an FEL operating in steady state is a monotonically increasing function of the detuning parameter, the same argument leads to the

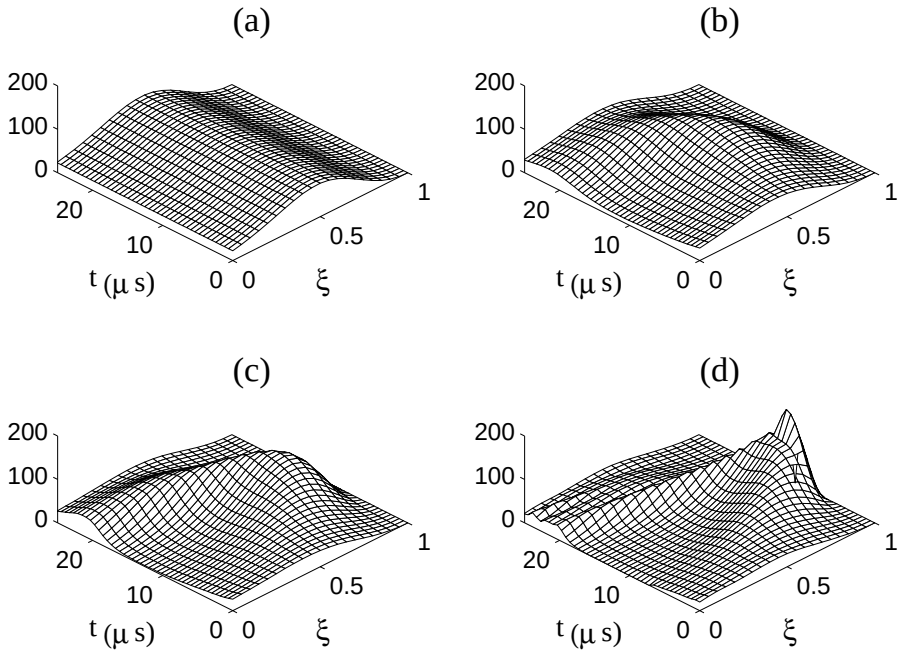

FIG. 6. Optical amplitude $|A(\xi,\tau)|^2$ vs ξ and time (one period of beam energy modulation) at different modulation amplitudes: (a) $\Delta\nu_m = 0$, (b) $\Delta\nu_m = 0.01$, (c) $\Delta\nu_m = 0.022$, and (d) $\Delta\nu_m = 0.0345$. The average cavity detuning is $\nu_0 = 0.03$.

expectation that the micropulse length will get longer (shorter) as $\nu > \nu_0$ ($\nu < \nu_0$). Even though for small ν the micropulse length is proportional to $\nu^{1/3}$ [7], a practical lower limit to attainable equilibrium micropulse lengths is set by the requirement that $\nu > \nu_{\max}$ (to maintain oscillation). Under the dynamic conditions present with modulated desynchronism, the requirement for FEL operation is modified. It is all right for ν to be less than $\nu_{\max}$ (where the gain is less than the loss), or even for ν to be less than zero (where gain as conventionally defined does not exist), for a short time. Soon after the time that ν is in this normally inaccessible region ($\nu < \nu_{\max}$), the micropulse energy will certainly begin to decay. But as long as ν returns to the conventional region ($\nu > \nu_{\max}$) soon enough, and remains there long enough, it is reasonable to assume that the micropulse energy will remain significant throughout the entire process.

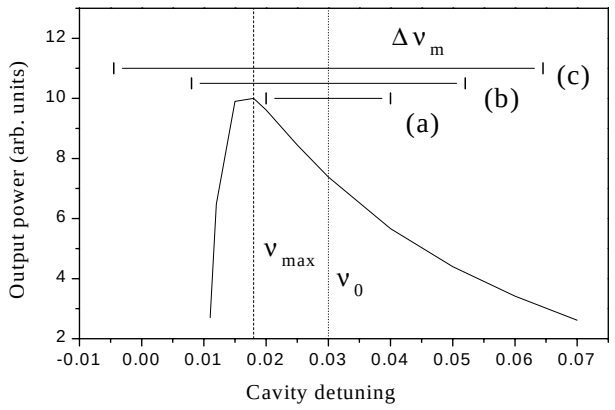

FIG. 7. Output power versus cavity detuning. The modulation amplitudes (a) $\Delta\nu_m = 0.01$, (b) $\Delta\nu_m = 0.022$, and (c) $\Delta\nu_m = 0.0345$ used in the simulation, the average cavity detuning $\nu_0 = 0.03$ (dotted line), and the maximum power cavity detuning $\nu_{\max}$ (dashed line) are shown.

It is difficult to state in detail what will happen to the micropulse while $\nu < \nu_{\max}$. However, keeping in mind the fact that there is still an interaction between the electron microbunch and the FEL micropulse, general considerations make it clear that there will be a strong tendency for all of the optical energy to concentrate at the trailing edge of the electron bunch [5]. This makes it plausible that the micropulse length decreases while $\nu < \nu_{\max}$, but answers to questions such as the total micropulse energy and the actual micropulse length require numerical calculation. Interestingly enough, although the normally defined gain in the inaccessible region is (by definition) less than the cavity losses, calculations using a step function detuning show that it is perfectly possible for the micropulse energy to show a brief increase when entering the region.

Finally, we study the effect of changing the modulation frequency. The time averaged optical power P_t and the minimum micropulse length $L_{\min}$ are plotted (for $\Delta\nu_m = 0.0345$) as a function of the modulation frequency in Fig. 8. There is a general trend toward larger P_t as f_m becomes larger, suggesting a slight bias toward operating at higher modulation frequencies. On the other hand, the minimum pulse length shows a rather rapid change in magnitude around 45 kHz. For $f_m < 40$ kHz the pulse length

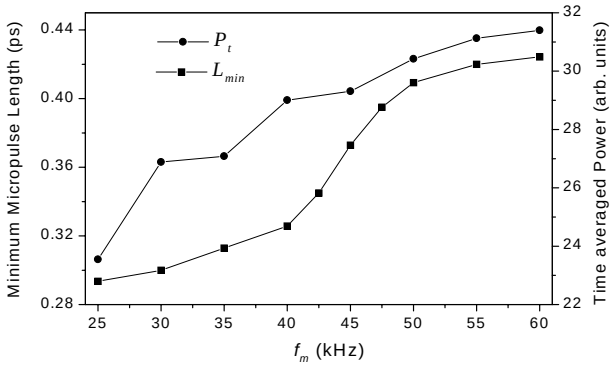

FIG. 8. Minimum micropulse length $L_{\min}$ (squares) and time averaged power P_t (circles) versus the modulation frequency f_m for $\Delta\nu_m = 0.0345$. The average cavity detuning is $\nu_0 = 0.03$.

remains almost constant at around 300 fs, while above 50 kHz it is about 400 fs. The optimum frequency for obtaining short pulse with high power is therefore around 40 kHz, a result which agrees with our experimental observations.

It is interesting to note that, if our system is simulated with $\alpha_0 = 0.016$ (a reduction of about a factor of 2 from our actual system), our FEL enters the well-known limit cycle [3,7] regime and oscillates at about 40 kHz (see Fig. 9). It is tempting to imagine a connection between the optimum modulation frequency for the dynamic desynchronism and the limit cycle frequency. This interpretation receives some support from the recent results of Jaroszynski *et al.* [12] in which they observed resonances in the behavior of their FEL when they modulated its desynchronism parameter at the limit cycle frequency and some of its multiples. Since the limit cycle frequency is a function of ν_0, the average desynchronism, the optimum modulation frequency, might also be expected to be a function of ν_0. We have not yet explored this possibility.

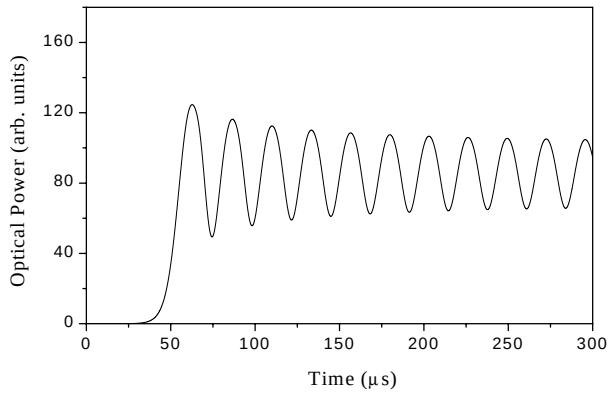

FIG. 9. Time evolution of the output power P for a small loss $\alpha_0 = 0.016$ and the same cavity detuning as in the previous simulation ($\nu = 0.03$) without modulated desynchronism.

D. Effect of the second derivatives terms

In this section we briefly discuss the effect of the second derivative terms that we introduced in the theoretical model [Eq. (3.1)]. For a direct comparison, the curves of Fig. 10 are exactly the same as those of Fig. 5, except that the second order terms have been ignored in Fig. 10. Comparing both figures with Fig. 1, it is evident that the curves of Fig. 5 provide a substantially better match to experiment than those of Fig. 10, particularly at larger values of the modulation. It is also interesting to note that the unmodulated reference curves on Fig. 10 are about 25% lower than those on Fig. 5. This effect of the second order terms was not anticipated.

To quantify the importance of the second order terms, we define a parameter

$$\Gamma(\tau) = \frac{\frac{1}{4}\int_0^1 d\xi \left|\frac{\partial^2 A}{\partial \tau^2}\right|^2}{\frac{1}{4}\int_0^1 d\xi \left|\frac{\partial^2 A}{\partial \tau^2}\right|^2 + \int_0^1 d\xi \left|\frac{\partial A}{\partial \tau}\right|^2} \tag{3.10}$$

that measures the relative importance of the second order terms to the first order terms. For small modulation amplitudes, the contribution of the second order terms vanishes. Figure 11 shows the time evolution of Γ for $\Delta\nu_m = 0.0345$ and $\nu_0 = 0.03$, along with the cavity detuning and the cavity power. An examination of the figure shows that the second order terms seem to be important

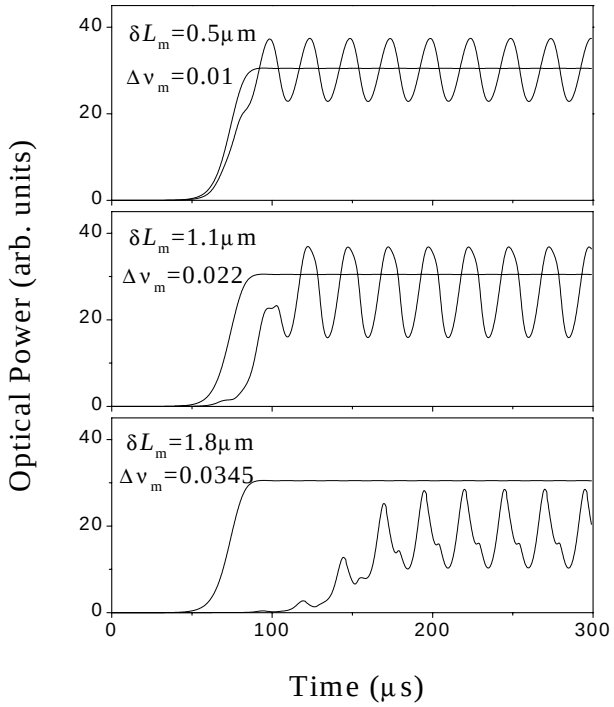

FIG. 10. Optical power signal as a function of time with different levels of cavity detuning modulation for the case without second derivative terms. The flat curves are for situations without the energy modulation. The average cavity detuning is $\nu_0 = 0.03$.

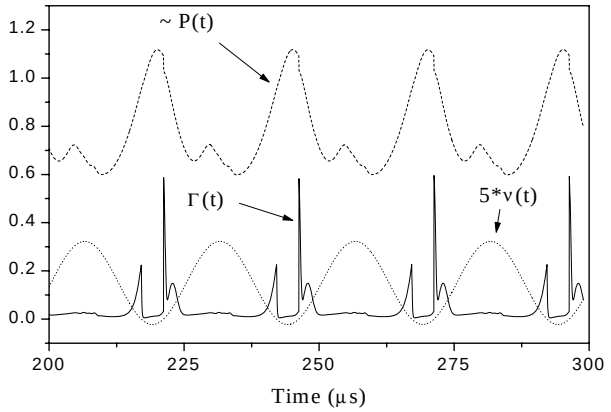

FIG. 11. Time evolution of Γ for $\Delta\nu_m = 0.0345$ (solid line). The time evolution of the rescaled power ($\propto P$) (dashed line) and the cavity detuning (5ν) (dotted line) are also shown. The average cavity detuning is $\nu_0 = 0.03$.

only for brief periods when the cavity length is changing rapidly while it is less than $\nu_{\max}$ ($\simeq 0.017$). However, during those periods the second order terms can dominate the first order terms.

IV. CONCLUSIONS

We have studied the effect of desynchronism modulation on short pulse free-electron laser oscillators. Desynchronism modulation is achieved experimentally by modulating the energy of the electron beam that passes through a nonisochronous magnetic chicane in the FEL beam line. We find that the output power and the micropulse length of the FEL beam oscillate periodically at the modulation frequency and that the minimum micropulse length during the cycle can be significantly shorter than that which can be obtained without modulation. For example, when the desynchronism of our FEL is modulated at 40 kHz, the minimum measured micropulse length is 300 fs. Without modulation the minimum is about 700 fs.

The experimental results have been reproduced theoretically using the short pulse FEL oscillator equations [7,8,13], retaining two terms that are usually discarded and that are relevant in explaining the behavior of the system when the cavity detuning is very small or negative and is changing rapidly. We have found that when the desynchronism is modulated, the FEL can operate for part of the cycle in the normally inaccessible portion of the output power curve where the FEL gain is less than the cavity losses. It is even possible for the FEL to operate periodically in the region of negative desynchronism where gain, as normally defined, does not exist.

This work was supported in part by ONR Grant No. N000140-94-1-1024 and by Universidad Complutense de Madrid.

[1] G. Dattoli and A. Renieri, in *Experimental and Theoretical Aspects of the Free-Electron Laser,* edited by M. L. Stitch and M. Bass, Laser Handbook Vol. 4 (North-Holland, Amsterdam, 1985), p. 1.
[2] D. A. Jaroszynski, P. Chaix, N. Piovella, D. Oepts, G. M. H. Knippels, A. F. G. van der Meer, and H. H. Weits, Phys. Rev. Lett. **78**, 1699 (1997).
[3] D. A. Jaroszynski, R. J. Bakker, A. F. G. van der Meer, D. Oepts, and P. W. van Amersfoort, Phys. Rev. Lett. **70**, 3412 (1993).
[4] R. J. Bakker, G. M. H. Knippels, A. F. G. van der Meer, D. Oepts, D. A. Jaroszynski, and P. W. van Amersfoort, Phys. Rev. E **48**, R3256 (1993).
[5] N. Piovella, Phys. Rev. E **51**, 5147 (1995).
[6] G. Shvets and J. S. Wurtele, Phys. Rev. E **56**, 3606 (1997).
[7] N. Piovella, P. Chaix, G. Shvets, and D. A. Jaroszynski, Phys. Rev. E **52**, 5470 (1995).
[8] P. Chaix, N. Piovella, and G. Gregoire, Phys. Rev. E **59**, 1136 (1999).
[9] T. I. Smith, in *Proceedings of the 19th International Free Electron Laser Conference, Beijing, 1997*, edited by Jialin Xie and Xiangwan Du (Elsevier, Amsterdam, 1998).
[10] T. I. Smith and T. Kimura, in *Proceedings of the 20th International Free Electron Laser Conference, Williamsburg, Virginia, 1998,* edited by G. R. Neil and S. V. Benson (Elsevier, Amsterdam, 1999).
[11] D. A. Jaroszynski, A. F. G. van der Meer, P. W. van Amersfoort, and W. B. Colson, Nucl. Instrum. Methods Phys. Res., Sect. A **296**, 480 (1990).
[12] D. A. Jaroszynski, D. Oepts, A. F. G. van der Meer, and P. Chaix, Nucl. Instrum. Methods Phys. Res., Sect. A **407**, 407 (1998).
[13] R. Bonifacio, F. Casagrande, and L. De Salvo Souza, Phys. Rev. A **33**, 2836 (1986).